THE JOURNAL OF BIOLOGICAL CHEMISTRY VOL. 287, NO. 46, pp. 39083–39093, November 9, 2012

The Kelch Protein KLHDC8B Guards against Mitotic Errors, Centrosomal Amplification, and Chromosomal Instability[S]

Received for publication, June 12, 2012, and in revised form, September 13, 2012 Published, JBC Papers in Press, September 17, 2012, DOI 10.1074/jbc.M112.390088

Maxwell M. Krem[1], **Ping Luo, Brandon I. Ing, and Marshall S. Horwitz**

From the Department of Pathology and the Institute for Stem Cell and Regenerative Medicine, University of Washington School of Medicine, Seattle, Washington 98109

Background: The large multinucleated Reed-Sternberg cell is the driving force behind Hodgkin lymphoma pathogenesis.
Results: Disrupting KLHDC8B function leads to multinucleation, failed mitoses, centrosomal amplification, and aneuploidy, the major pathologic features of the Reed-Sternberg cell.
Conclusion: KLHDC8B protects against mitotic errors and chromosomal instability.
Significance: Midbody proteins play a previously unappreciated key role in Hodgkin lymphoma pathogenesis.

The malignant cell in classical Hodgkin lymphoma (HL) is the binucleated giant Reed-Sternberg cell. Chromosomal instability and mitotic errors may contribute to HL pathogenesis; one potential mitotic regulator is the kelch protein KLHDC8B, which localizes to the midbody, is expressed during mitosis, and is mutated in a subset of familial and sporadic HL. We report that disrupting KLHDC8B function in HeLa cells, B lymphoblasts, and fibroblasts leads to significant increases in multinucleation, multipolar mitoses, failed abscission, asymmetric segregation of daughter nuclei, formation of anucleated daughter cells, centrosomal amplification, and aneuploidy. We recapitulated the major pathologic features of the Reed-Sternberg cell and concluded that KLHDC8B is essential for mitotic integrity and maintenance of chromosomal stability. The significant impact of KLHDC8B implicates the central roles of mitotic regulation and chromosomal segregation in the pathogenesis of HL and provides a novel molecular mechanism for chromosomal instability in HL.

Hodgkin lymphoma (HL)[2] accounts for 11% of new lymphoma diagnoses in the United States (1). The pathologic hallmark of HL is the multinucleated giant Reed-Sternberg (RS) cell. Morphologically, RS cells are scant in number and are surrounded by nonclonal lymphocytes and other reactive cells. In recent years, the RS cell has been determined to be a B cell of germinal center origin (2, 3), as demonstrated by the presence of rearranged and somatically mutated immunoglobulin variable region genes (4–6). The multinucleated appearance of RS cells is thought to be attributable to a disturbance in cytokinesis, rather than cell fusion, by mononuclear Hodgkin cells (7–10).

Some of the most conspicuous mutations in HL are chromosomal aberrations; case series show strong evidence of chromosomal instability and chromosomal aberrations in most cases of HL (11, 12), where there is a particularly heavy frequency of tetraploidy or near-tetraploidy (13, 14). It has been speculated that RS cells or their immediate precursors are derived from a karyotypically aberrant lineage (2). Amplification of the number of centrosomes is implicated in polyploidy in both classical HL cell lines and patient cases (15–17). Centrosomal amplification has been linked to chromosomal instability, as extra centrosomes promote chromosomal missegregation during cell division (18); such phenomena could be related to altered expression of spindle checkpoint genes (19). Telomere dysfunction in Hodgkin cells is also believed to lead to complex karyotypes and genetic instability, leading to a transition to RS cells (20, 21). Nevertheless, the mechanisms underlying chromosomal instability in HL remain only partially explored.

We recently reported a candidate gene for the role of mitotic regulator in HL (22). A familial balanced translocation between chromosomes 2 and 3 resulted in classical HL occurring in several different family members due to interruption of *KLHDC8B* on chromosome 3, which encodes a midbody kelch domain protein expressed during mitosis. Additionally, a single nucleotide polymorphism in the 5′-untranslated region of the gene, which was associated with reduced translation, was also associated and linked with HL in other families. We also identified acquired loss of heterozygosity in a sporadic case of HL. Taken together, the genetic data provide compelling evidence that KLHDC8B participates in lymphomagenesis. Kelch proteins are known to facilitate protein-protein interactions and play key roles in cell division (23), yet despite the new insights from mutation of KLHDC8B, the mechanism of its function and molecular consequences of its dysfunction are unknown.

Here, we investigate the role of the HL-related protein KLHDC8B. We interfered with the function of KLHDC8B by both stable knockdown and expression of a dominant-negative KLHDC8B-GFP fusion protein. We generated multinucleated lymphoblasts that mimic the appearance of the RS cell. Video microscopy revealed the aberrant mitotic mechanisms by which multinuclear cells are generated, and we showed that loss

[S] This article contains supplemental Movies 1–6 and Figs. 1–4.

[1] Recipient of funding from the Leukemia and Lymphoma Society, the Conquer Cancer Foundation of the American Society of Clinical Oncology, and the St. Baldrick's Foundation. To whom correspondence should be addressed: Institute for Stem Cell and Regenerative Medicine, Campus Box 358056, University of Washington School of Medicine, 850 Republican St., Seattle, WA 98109. Tel.: 206-616-4567; Fax: 206-897-1775; E-mail: mkrem@u.washington.edu.

[2] The abbreviations used are: HL, Hodgkin lymphoma; KLHDC8B, Kelch-like domain-containing protein 8B; RS, Reed-Sternberg; FuKG, fusion of KLHDC8B and GFP.

of KLHDC8B function induces centrosomal amplification and aneuploidy, key pathologic characteristics of RS cells. Thus, we demonstrate that KLHDC8B is essential for mitotic integrity and maintenance of chromosomal stability and that loss of KLHDC8B recapitulates the major pathologic features of HL.

EXPERIMENTAL PROCEDURES

Plasmid Constructs—The tetracycline-inducible, stably transfectable anti-KLHDC8B short hairpin RNA plasmid was generated as follows. We amplified the short hairpin RNA (shRNA) from the vector TI369558 (Origene) using the forward primer 5′-CTTGTGGAAAGGACGCGCTCGAGTGCTG-3′ and the reverse primer 5′-CACCCTAACTGACACACATTC-CACAGGG-3′. The shRNA segment was subcloned into the vector pSingle-tTS-shRNA (Clontech), which contains ampicillin and neomycin resistance markers. The shRNA plasmid TI369559 and noneffective GFP negative control vector TR30003 (Origene), both containing a kanamycin/puromycin selection cassette, were used without modification.

The stably transfectable expression vector for the fusion of KLHDC8B and *Aequorea coerulescens* GFP was generated by amplifying the cDNA of KLHDC8B with the forward primer 5′-TAGCTAGCCGAGGCGGAACGGCG-3′ and the reverse primer 5′-GTAAGCTTGACCCCACGCAGACACAG-3′. The ensuing product was subcloned in-frame into pAcGFP1-N1 (Clontech), resulting in the linker peptide RILQSTVPRARD-PPV followed by the GFP domain at the C terminus of KLHDC8B.

Cell Culture—HeLa cells (ATCC) and the hTERT-immortalized human foreskin fibroblast line 82-6HT (kindly provided by P. Rabinovitch) were cultured in DMEM supplemented with 15% fetal calf serum (Invitrogen). HeLa cells were transfected using Lipofectamine and Plus reagents (Invitrogen). Stable HeLa clones were selected by plating serial dilutions and growing with medium containing 200 μg/ml G418 (Invitrogen). 82-6HT cells were transfected with an Amaxa device, utilizing Nucleofector Solution V (Lonza). Stable 82-6HT clones were selected by plating serial dilutions and grown in medium containing 0.5 μg/ml puromycin. Surviving colonies were harvested by trypsinizing within metal cylinders.

HMy2.C1r (ATCC) and T5-1 (kindly provided by K. Muczynski) B lymphoblastoid cells were cultured in RPMI medium supplemented with 10% fetal calf serum. Lymphoblasts were transfected with an Amaxa device, utilizing Nucleofector Solution C (Lonza). HMy2.C1r clones were plated at serial dilutions and grown in medium containing 400 μg/ml G418. T5-1 clones were plated at serial dilutions, over an irradiated feeder layer of 82-6HT cells, with medium containing 0.25 μg/ml puromycin.

Antibodies, Western Blotting, and Immunohistochemistry—Chicken polyclonal IgY antibodies were raised against KLHDC8B as described previously (22). Cell extracts were prepared using a hypotonic lysis buffer supplemented with protease inhibitors (complete Mini, Roche Applied Science). Proteins were subjected to SDS-PAGE and blotted onto a PVDF membrane (Bio-Rad). Anti-KLHDC8B Western blots used a 1:10,000 dilution of primary antibody followed by a 1:10,000 dilution of horseradish peroxidase (HRP)-conjugated goat anti-chicken IgY secondary antibody (Aves), developed with the ECL Western blotting detection kit (Amersham Biosciences). Anti-GFP Western blots used a 1:200 dilution of rabbit polyclonal antibody SC-8334 (Santa Cruz Biotechnology), followed by a 1:5000 dilution of horseradish peroxidase (HRP)-conjugated goat anti-rabbit IgG secondary antibody SC-2054 (Santa Cruz Biotechnology), developed with the ECL kit as above. Actin loading control was detected with the C-11 HRP-conjugated antibody (Santa Cruz Biotechnology) at 1:1000 dilution.

For immunofluorescence staining, cells were fixed in methanol-free 4% formaldehyde and permeabilized with 0.1% Triton X-100. Blocking was with 0.5% BSA. We used a 1:10,000 dilution of anti-KLHDC8B antibody, 1:1000 dilution of rabbit anti-pericentrin antibody ab4448 (Abcam), and 1:500 dilution of mouse anti-α-tubulin antibody ab7291 (Abcam) for the primary antibodies. This was followed by a 1:1000 dilution of Alexa Fluor 555-labeled goat anti-chicken, 1:1000 Alexa 594-labeled donkey anti-rabbit, and 1:500 Alexa Fluor 555-labeled goat anti-mouse secondary antibodies (Invitrogen) for KLHDC8B, pericentrin, and α-tubulin, respectively. 4′,6-Diamino-2-phenylindole (DAPI) was used for nuclear counterstaining. Images were obtained with a Zeiss Axioplan fluorescence microscope and a Nikon A1R confocal laser scanning microscope, using NIS Elements acquisition software.

Cell Counting and Multinucleation Analysis—HeLa and 82-6HT cells were plated at low density to coverslips, followed by formaldehyde fixation as above. Nuclei were stained with DAPI. Cells were counted manually using a Zeiss Axioplan fluorescence microscope using both fluorescence and differential interference contrast microscopy. HMy2.C1r and T5-1 lymphoblasts were cultured to a density no greater than 500,000 cells/ml, spun onto poly-L-lysine-coated slides (Thermo), and subjected to Wright staining with the Hema 3 kit (Fisher). Cells were defined as multinuclear if two or more nuclei were contained within the border of a single cell.

Live Cell Imaging—HeLa cell lines were plated at low density to 6-well plates. For live cell imaging, cells were cultured in DMEM devoid of phenol red, supplemented with 15% fetal calf serum. DNA was labeled with 0.8 μM Hoechst stain for 20 min prior to imaging. Images were obtained with a Nikon TiE inverted fluorescence microscope equipped with an incubator to maintain cells at 37 °C in 5% carbon dioxide. Images were recorded every 4 min over 16–24-h periods in the differential interference contrast, GFP, and DAPI channels, with exposure times and gains adjusted to minimize exposure to ultraviolet light. Acquisition software was NIS Elements. Mitoses of mononuclear cells were considered to be aberrant if the result was anything other than two mononuclear cells. Mitoses of multinuclear cells were considered to be neither normal nor aberrant. Mitoses were considered to start with regression of the cell membrane (release of surface attachments) and were considered to end when the midbody bridge resolved or, in the case of failed cytokinesis, when the daughter cell membrane stabilized. The above timeline definitions were chosen based on the known midbody localization of KLHDC8B and its effect on multinucleation. Boundaries between mitotic phases were defined as follows: the end of prophase occurred with maximum condensation of chromosomes; the end of metaphase occurred with separation of chromosomes; the end of anaphase

occurred with formation of a cleavage furrow; and the end of telophase occurred with stabilization of the nuclear membranes. We reasoned that mitotic timeline definitions based on cell sorting-measured transitions were not fully applicable to our imaging modality; furthermore, such boundaries are also fraught with subjectivity (24). The supplemental movies were generated with the Nikon Elements software package.

Karyotyping and Fluorescence in Situ Hybridization (FISH)—Cytogenetic analyses were performed with the assistance of the University of Washington Cytogenetics Laboratory. To obtain karyotypes, Giemsa banding was performed, with examination of five metaphases. For FISH, exponentially growing cells from each clone were incubated starting at a density of 4×10^5 cells/ml at 37 °C for 24 h, after which time colcemid was added to a final concentration of 0.2 mM to arrest the cells in metaphase. Cells were harvested 2 h later by centrifugation, and slides were prepared from the fixed cell suspensions. Fixed nuclei were stained with AneuVysion probes specific for chromosomes 13 and 21 (Abbott) and counterstained with DAPI.

Statistics—The p values for multinucleation assays are derived from two-tailed, two-sample t tests assuming equal variances. The p values for micronucleation and aneuploidy assays are derived from two-tailed, two-sample χ^2 tests using the Fisher exact test.

RESULTS

Stable KLHDC8B Knockdown Produces a Multinucleation Phenotype—Patients with familial classical HL due to a balanced translocation between chromosomes 2 and 3 have haploinsufficiency of *KLHDC8B*, which is predicted to lead to constitutive but partial loss of protein expression. We replicated that disease scenario with stable but partial knockdown in human cell line models. We stably transfected HeLa cells with a tetracycline-inducible shRNA ("shRNA1") construct targeting *KLHDC8B*. Based on Western blot analysis of KLHDC8B expression, we generated two derivative cell lines with partial knockdown upon doxycycline induction (Fig. 1*A*). The cell lines demonstrate an increased number of multinucleated (defined as two or more nuclei) cells upon doxycycline administration (Fig. 1, *B* and *C*) for 72 h, corresponding to ~3 cell generations. The effect is maintained after 144 h of doxycycline induction, suggesting that prolonged partial loss of expression leads to a stable multinucleation phenotype.

We used the same construct to stably transfect the human B lymphoblastoid cell line HMy2.C1r (25). After cloning by limiting dilution and Western blot assessment of protein expression, we produced a derivative cell line with partial KLHDC8B knockdown (Fig. 1*D*). As seen with HeLa, more than one band was sensitive to doxycycline induction, suggesting that the multiple bands may result from a post-translational modification. The knockdown line demonstrated increased numbers of multinucleated cells (Fig. 1*E*). The morphology of the multinucleated cells is reminiscent of the Reed-Sternberg cell, with copious cytoplasm and vacuolization (Fig. 1*F*).

KLHDC8B-GFP Fusion Protein Disrupts Cytokinesis—We sought to further explore the role of KLHDC8B in cytokinesis and multinucleation by generating a green fluorescent protein (GFP) fusion construct, suitable for *in vivo* cell imaging. We placed the GFP domain at the C terminus to avoid disruption of the KLHDC8B-sensitive 5′-untranslated region, point mutation of which influences translational efficiency and is associated with HL (22). We transiently transfected HeLa cells with an expression plasmid encoding the fusion construct of KLHDC8B and GFP (FuKG). Western blotting of lysates for both KLHDC8B and GFP confirmed the predicted protein's molecular mass of 65 kDa (Fig. 2*A*). We also transfected HeLa with the same plasmid, selected for stable transfectants with G418, and we used Western blotting for GFP to select derivative lines that stably expressed FuKG.

Surprisingly, HeLa cells transiently transfected with *FuKG* had a multinucleation rate approximately three times greater than baseline (Fig. 2*B*). Confocal microscopy with immunostaining for KLHDC8B, GFP fluorescence, and DAPI staining of DNA revealed occasional post-mitotic cell pairs with agglomerations of fusion protein between daughter cells or embedded within multinucleated cells (Fig. 2*C*). Chromosome-like material, stained with DAPI, was stranded between the daughter cells or nuclei (supplemental Fig. 1). Thus, FuKG has the unanticipated ability to interfere with midbody function and appears to function as a dominant-negative form of KLHDC8B, in the sense that it disrupts function by the presence of small quantities that antagonize the normal function of the wild-type protein.

We generated stably transfected HeLa lines expressing FuKG to better explore the mitotic effects of interfering with KLHDC8B's function. Stable expressors of FuKG were selected by Western blot screening of cell lysates for KLHDC8B and GFP (Fig. 2*A*). Stable transfectants expressed lower quantities of FuKG protein than transient transfectants. We surmised that high levels of FuKG expression were toxic and interfered with cell line viability. Stable expression of FuKG (clones 10 and 19) induced the highest rates of multinucleation that we had observed, up to 14%. As controls, we utilized untransfected HeLa and derivative clones (clones 1 and 22) that demonstrated G418 resistance but no detectable FuKG expression by Western blot (Fig. 2*D*). Confocal imaging of the stable expressors once again revealed the presence of fusion protein aggregates (Fig. 2*E*). We found that the presence of GFP-fluorescing aggregates was statistically associated with the characteristics of multinucleation (Table 1), supporting the argument that interfering with KLHDC8B function contributes to multinucleation. Our imaging experiments uncovered an increased presence of micronuclei in cell lines expressing FuKG, suggesting that the fusion protein additionally contributes to missegregation of chromosomes (Table 2).

To assess the impact of KLHDC8B on the mitotic spindle, we performed confocal imaging with immunofluorescence directed against α-tubulin. Stable FuKG expressors showed fraying of microtubules and an increased propensity to form multipolar spindles, although inadequate numbers of spindles were available for statistical analysis (supplemental Fig. 2).

We performed live cell fluorescent video microscopic observations of the two *FuKG* stable transfectant lines to explore how the dominant-negative fusion protein caused multinucleation. Three control cell lines were utilized (two FuKG nonexpressors and untransfected HeLa) to evaluate for the effects of UV expo-

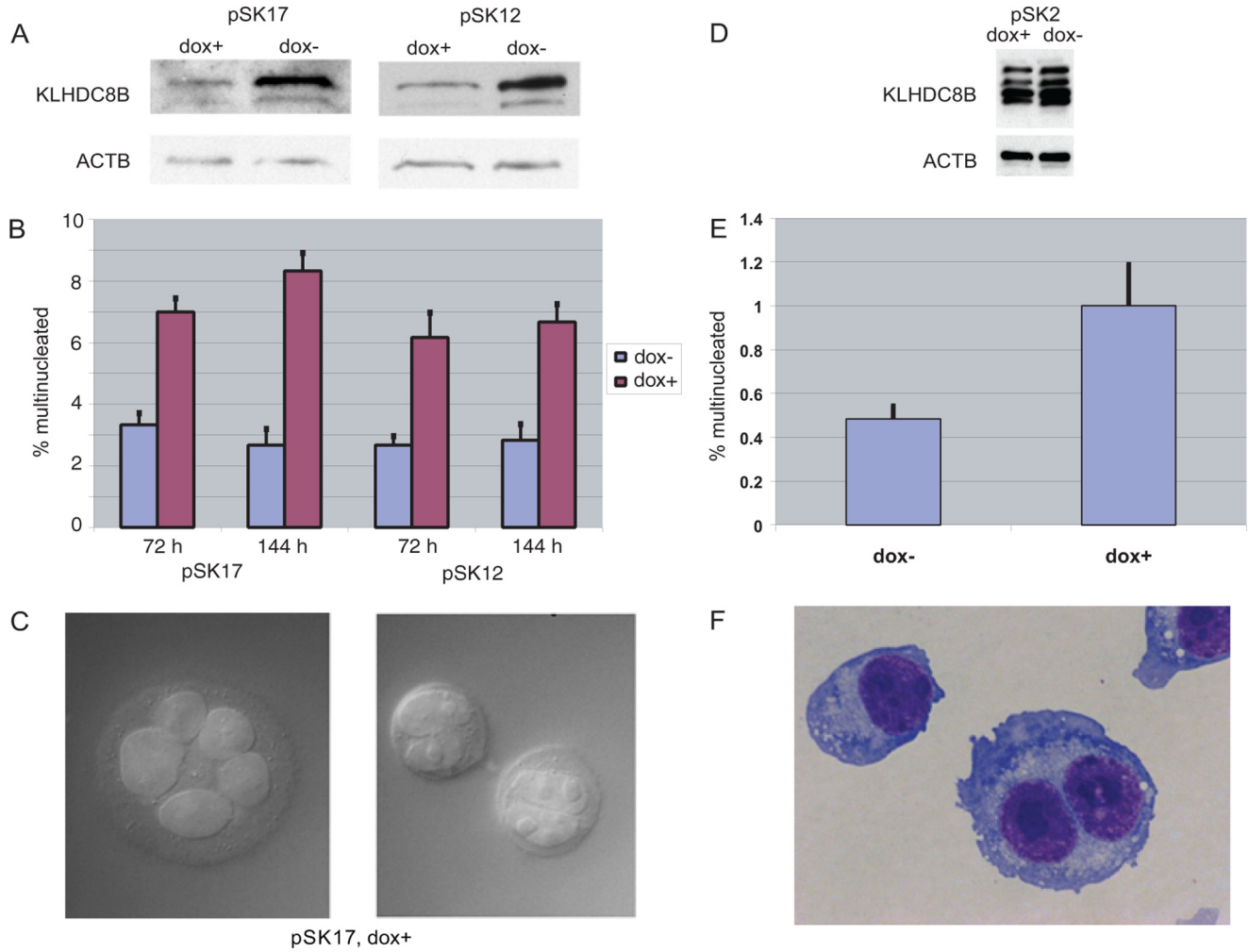

FIGURE 1. **Partial but stable knockdown of KLHDC8B induces a multinucleation phenotype.** *A,* Western blotting of KLHDC8B knockdown in HeLa stable transfectants pSK12 and pSK17. Knockdown was induced using the tetracycline-responsive vector pSingle-tTS-shRNA carrying anti-KLHDC8B shRNA. Cells were plated at low density to ensure optimal growth and harvested at 72 h. *B,* multinucleation in the presence (*crimson*) and absence (*blue*) of KLHDC8B knockdown induction. Three experiments were performed. Cells were plated at low density and fixed after 72 and 144 h. 600 cells were counted in each experimental arm. Statistical significances for multinucleation are as follows: pSK17, 72 h, $p = 0.0031$; pSK17, 144 h, $p = 0.0019$; pSK12, 72 h, $p = 0.0147$; pSK12, 144 h, $p = 0.0079$. *C,* multinucleated cells of clone pSK17. *D,* Western blotting of KLHDC8B knockdown in the HMy2.C1R clone pSK2, carrying pSingle-tTS-shRNA with anti-KLHDC8B shRNA. Cells were subcultivated at low density to ensure optimal growth and harvested at 72 h. *ACTB,* β-actin. *E,* multinucleation occurred when KLHDC8B knockdown was induced by doxycycline (*dox*) after 72 h of growth. Three experiments were performed, with 2000 cells counted for each condition, $p = 0.058$. *F,* multinucleated lymphoblasts under KLHDC8B knockdown demonstrate vacuolation and extensive cytoplasm, similar to the pathologic RS cells of HL.

sure and DNA labeling on cell division. We did not observe any cell fusion events for the expressor lines FuKG10 ($n = 375$) or FuKG19 ($n = 283$), supporting our working hypothesis that KLHDC8B disruption induces multinucleation through disruption of cytokinesis. We defined aberrant mitoses of mononuclear cells as those resulting in an outcome other than two mononuclear daughter cells (Fig. 3*A*). The FuKG expressor lines demonstrated increased rates of aberrant mitoses compared with nonexpressor and untransfected controls (Fig. 3*B*). Peri-mitotic blebbing was a frequent observation in expressor cell lines. Among aberrant mitoses, failed abscission events (inability to initiate or complete a cleavage furrow) were most common; there were also high rates of anucleate cell generation and multipolar mitoses, occasionally with generation of three daughter cells (Table 3 and supplemental Movies 1–5).

FuKG expressors demonstrated a longer average duration of mitosis, with abnormal mitoses accounting exclusively for the difference in the length of time required to complete mitosis (Fig. 3*C*). This suggests that the abnormal mitoses induced by the fusion protein are qualitatively different somehow from mitotic errors that would be present at baseline. We arbitrarily culled 62 mitoses (29 normal, 33 aberrant) from two separate live cell imaging experiments on line FuKG10 for detailed analysis of mitotic phase times. We found that prophase, metaphase, and anaphase were not statistically prolonged for aberrant mitoses. However, cytokinesis duration was roughly tripled, and telophase demonstrated a statistically significant but minor prolongation (Fig. 3*D*). Among the 33 aberrant mitoses, the phase of failure was distributed as follows: cytokinesis 16, telophase 10, anaphase 6, and metaphase 1.

Although FuKG expressor lines produced only small amounts of fusion protein, we recorded several instances of perimitotic fusion protein expression accompanied by aberrant mitoses (supplemental Fig. 3 and supplemental movie 6). Taken together, the results suggest that KLHDC8B is a key component

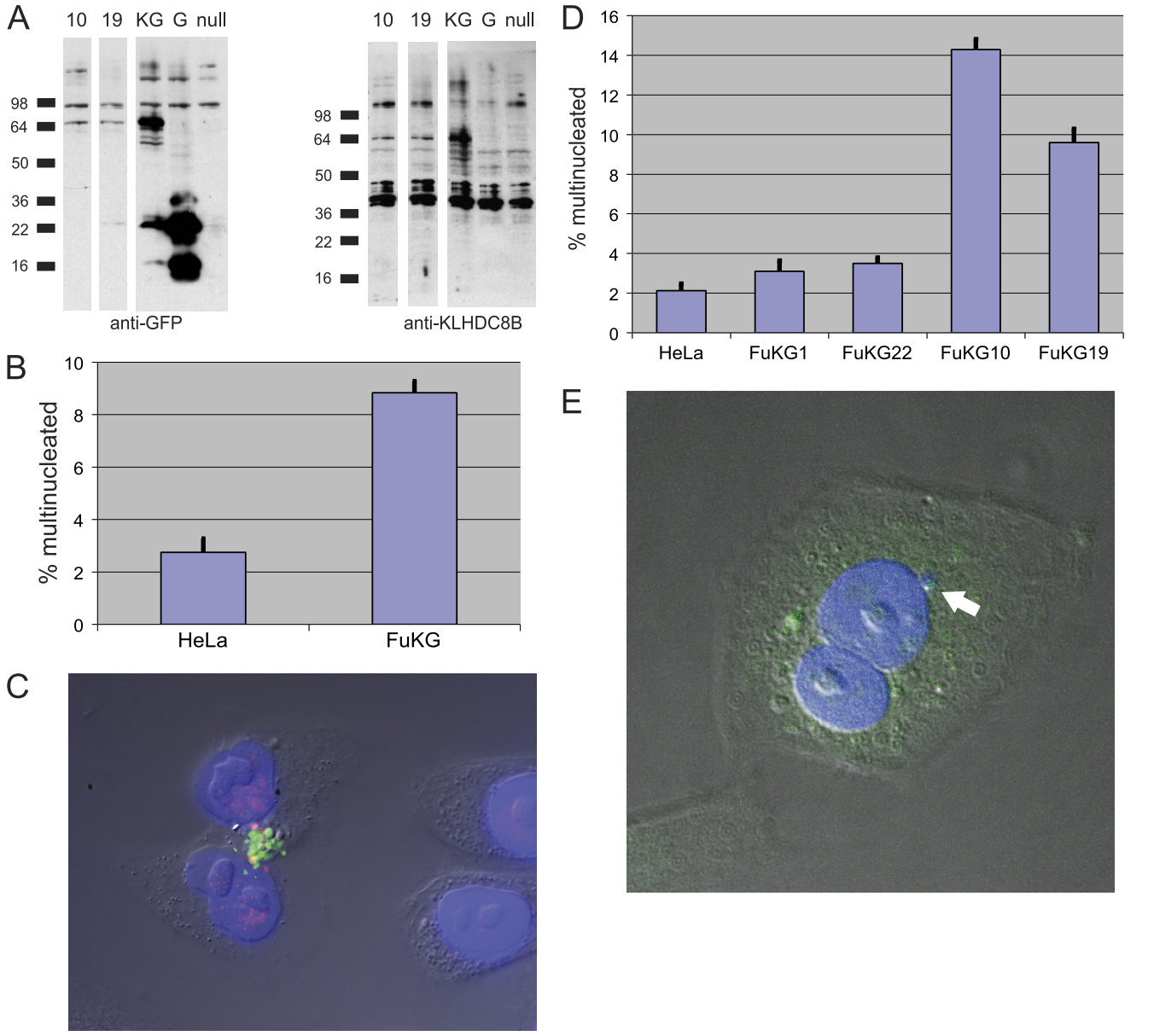

FIGURE 2. **Expression of KLHDC8B-GFP fusion protein (FuKG) is a potent inducer of multinucleation.** *A,* Western blotting of HeLa lysates with both anti-GFP and anti-KLHDC8B probing demonstrates expression of the expected 65-kDa fusion product. *Lane 10*, FuKG-stable transfectant clone 10; *lane 19*, FuKG-stable transfectant clone 19; *lane KG*, FuKG transiently transfected cells; *lane G*, GFP transiently transfected cells; *null*, untransfected HeLa control. In the case of transient transfectants, cells were harvested 48 h after transfection. *B,* multinucleation of untransfected HeLa controls ($n = 600$) and FuKG transient transfectants ($n = 800$), $p < 0.0001$. Cells were plated at low density to ensure optimal growth and harvested at 72 h. *C,* accumulation of FuKG fusion protein located centrally within a binucleate cell. Fluorescence microscopy shows FuKG fusion protein fluorescence (*green*), anti-KLHDC8B staining (*red*), and DNA staining with DAPI (*blue*). *D,* multinucleation of FuKG stable clones 10 ($n = 1400$) and 19 ($n = 1000$), compared with nonexpressor stable clones 1 ($n = 1000$) and 22 ($n = 600$), as well as untransfected HeLa ($n = 1600$). *E,* binucleated cell from line FuKG10, demonstrating fusion protein expression. The *white arrow* indicates a micronucleus.

TABLE 1
Correlation of green fluorescent aggregates with multinucleation

	Green aggregates	No aggregates	% incidence	*p* value
FuKG10				
Multinuclear	15	185	7.5	<0.0001
Mononuclear	5	1195	0.42	
FuKG19				
Multinuclear	6	90	6.25	0.0001
Mononuclear	4	900	0.44	

TABLE 2
Correlation of micronucleation with FuKG expression

	Micronuclei	No micronuclei	% incidence
HeLa	34	766	4.25
FuKG1	25	775	3.13
FuKG22	83	717	10.4
Total, controls	142	2258	**5.9**[a]
FuKG10	82	718	10.3
FuKG19	155	615	19.4
Total, FuKG expressors	237	1363	**14.8**[a]

[a] *p* value shows higher percentage of micronucleation in FuKG expressor cell lines *versus* control cell lines <0.0001 (boldface values).

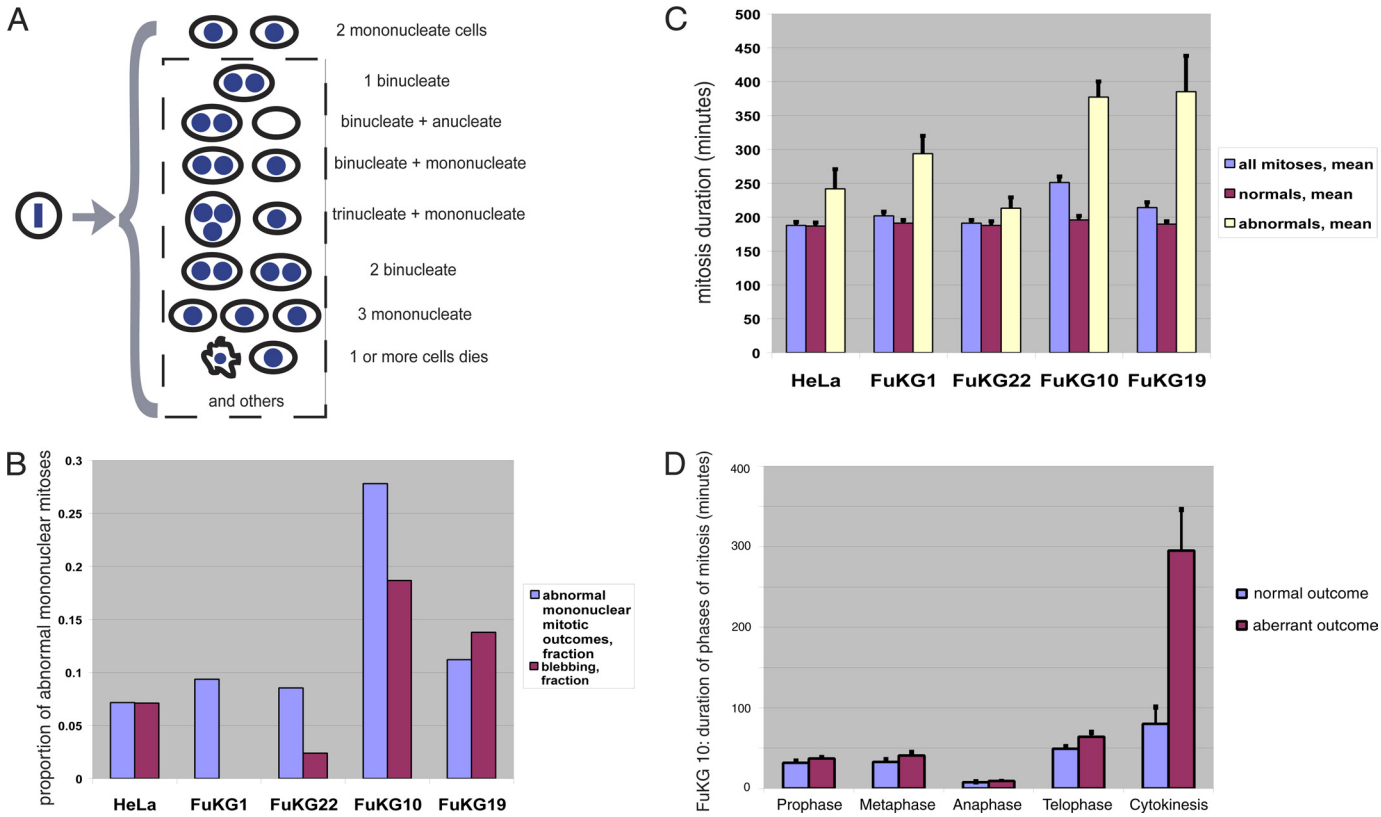

FIGURE 3. **Expression of FuKG disrupts mitosis.** *A,* schematic depicting possible mitotic results from a metaphase of a mononuclear cell division; the expected result is two mononuclear daughter cells, whereas all other outcomes (*dashed box*) are considered aberrant. *B,* video microscopic observation reveals that cell lines expressing the FuKG protein suffer from an increased rate of mononuclear cells undergoing abnormal mitotic events (mitotic product being any combination other than two mononuclear daughter cells or the presence of multiple cellular blebs forming during mitosis). Expressors were FuKG10 ($n = 360$) and FuKG19 ($n = 276$); controls were FuKG1 ($n = 96$), FuKG22 ($n = 82$), and HeLa ($n = 181$). *C,* cell lines expressing FuKG show an increase in the duration of mitosis, predominantly attributable to longer durations of abnormal mitoses. The duration of normal mitoses did not differ among the cell lines. For this calculation, binuclear cells undergoing symmetric segregation of nuclei were considered to be normal mitoses. FuKG10, $n = 375$; FuKG19, $n = 283$; FuKG1, $n = 98$; FuKG22, $n = 83$; HeLa, $n = 183$. *D,* frame-by-frame analysis of 29 mitoses with normal outcomes and 33 aberrant mitoses from line FuKG10. Durations of mitotic phases are indicated for normal (*blue*) and abnormal (*crimson*) mitoses. Prophase ($p = 0.13$), metaphase ($p = 0.10$), and anaphase ($p = 0.19$) showed nonsignificant trends toward prolongation, whereas telophase ($p = 0.023$) and cytokinesis ($p = 0.0004$) were statistically prolonged in aberrant mitoses.

TABLE 3
Aberrant mononuclear mitoses

	FuKG expressors	% of mononuclear mitoses	Controls	% of mononuclear mitoses	Total
1 nuc to 2 nuc	70	11	16	4.46	86
1 nuc to 2 nuc + anucleate	16	2.52	5	1.39	21
1 nuc to 2 nuc + 1 nuc	16	2.52	1	0.28	17
1 nuc to 1 nuc + anucleate	5	0.79	6	1.67	11
1 nuc to 3 nuc	7	1.1	0	0	7
1 nuc to 3 cells	6	0.94	0	0	6
1 or more cells die	5	0.79	1	0.28	6
1 nuc to 3 nuc + 1 nuc	1	0.16	1	0.28	2
1 nuc to 2 nuc + 2 nuc	2	0.31	0	0	2
1 nuc to 1 nuc	1	0.16	0	0	1
1 nuc to 3 nuc + anucleate	1	0.16	0	0	1

of midbody function, affecting not just abscission but also appropriate chromosomal and nuclear segregation.

KLHDC8B-GFP Fusion Protein Induces Centrosomal Amplification—Induction of tripolar mitoses and anucleate daughter cells suggested that KLHDC8B influences centrosome function. Therefore, we asked whether expression of the FuKG protein could induce centrosomal amplification. We assessed centrosome number and architecture by performing immunohistochemistry studies on stable HeLa expressors of FuKG, using antibodies against pericentrin, a centrosomal protein commonly used to visualize centrosomes. Control cell lines were the same as those used for the multinucleation and live cell imaging assays. The cell lines expressing the FuKG protein demonstrated marked increases in the number of cells with centrosomal amplification (three or more centrosomes) compared with controls (Fig. 4*A*). Among the cells with centrosomal amplification, three was the most common number; it is notable that even numbers of centrosomes were not predominant (Fig. 4*B*). We did not observe significant alterations in centrosomal architecture such as enlargement. Centrosomal amplification was strongly correlated with multinucleation, and

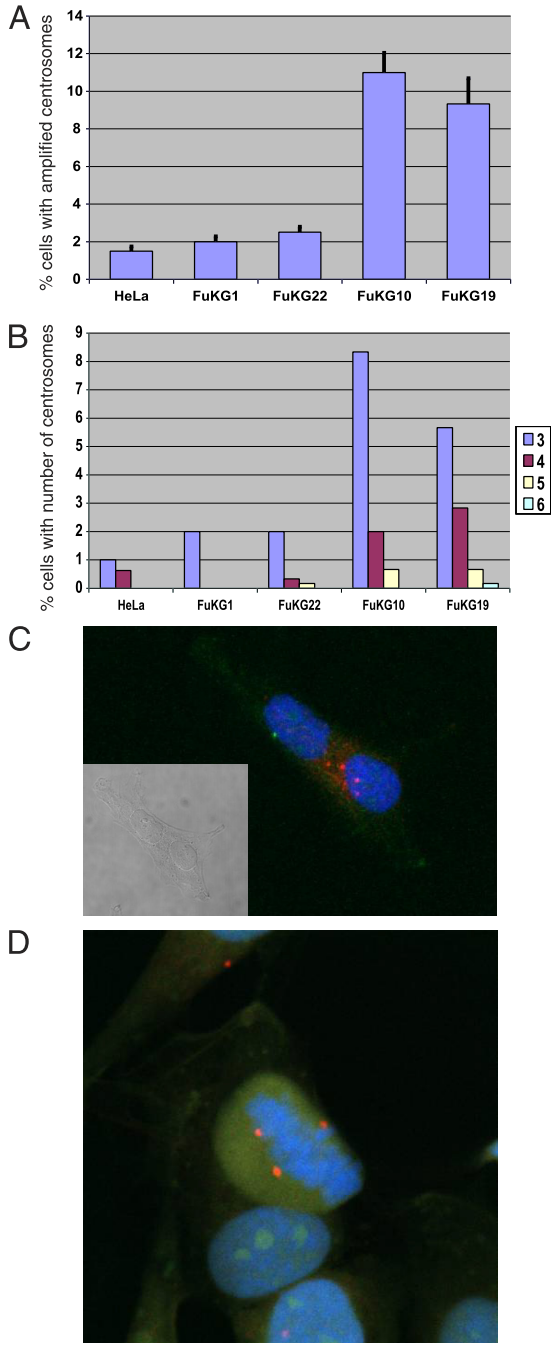

FIGURE 4. **Expression of FuKG induces centrosomal amplification.** *A,* fusion protein expressors and control lines were plated to coverslips at low density and grown for 48 h. Anti-pericentrin immunofluorescence was used to determine the number of centrosomes per cell. Cells with three or more centrosomes were considered to be have centrosomal amplification. 600 cells were counted for each line, with the exception of HeLa ($n = 800$). Fusion protein expressors FuKG10 and FuKG19 demonstrated significant centrosomal amplification. *B,* centrosomally amplified cells were categorized by the number of centrosomes in each cell. Greater numbers of centrosomes were associated with decreasing numerical frequency, suggesting that centrosomal amplification is not merely the result of duplication secondary to failed abscission events. *C,* representative cell with centrosomal amplification. The *inset* shows the differential interference contrast image of this binucleate cell. Confocal microscopy shows the staining for pericentrin (*red*) and DNA (*blue*), with expression of fusion protein (*green*) also present. The image shown is the composite overlay of a Z-stack of images. *D,* FuKG expressor cell with three centrosomes present at metaphase, rather than the expected two. Staining performed as in *C*. There is expression of fusion protein at the time of mitosis. Notably, centrosomal amplification is present prior to completion of mitosis.

greater numbers of nuclei appeared linked with greater numbers of centrosomes, although the size of the sample was inadequate for statistical analysis. However, expressor lines demonstrated an elevated incidence of centrosome amplification even in mononuclear cells (Table 4). Fig. 4, *C* and *D*, demonstrates centrosomal amplification in expressor lines, including a metaphase notable for three centrosomes and FuKG expression.

Stable KLHDC8B Knockdown Induces Aneuploidy—To investigate whether KLHDC8B protects against chromosomal instability, we sought diploid but transfectable and clonable cell lines. The B lymphoblastoid line T5-1 and the human foreskin fibroblast line 82-6HT met our requirements, with minor deviations from otherwise diploid karyotypes as follows: 46,XY,t(6;11)(p11;p11.1) for 82-6HT and 46,X,-X or -Y,dup(7)(q11.2q32) for T5-1. To confirm the knockdown phenotype, we determined whether T5-1 and 82-6HT would also be vulnerable to multinucleation after knockdown of KLHDC8B. For cytogenetic experiments, we utilized a puromycin-selectable, constitutively expressed shRNA ("shRNA3") with a more potent knockdown effect than the shRNA1 we used above, as shown previously by Salipante *et al.* (22). Stable transfectant clones of T5-1 and 82-6HT were derived and screened for KLHDC8B knockdown by Western blotting (Fig. 5*A*). We analyzed two lines each from T5-1 and 82-6HT that displayed increased multinucleation (Fig. 5*B*). Furthermore, immunostaining demonstrated that the two fibroblast lines have centrosomal amplification (supplemental Fig. 4).

We assessed chromosome segregation abnormalities by performing interphase FISH on chromosomes 13 and 21. Both chromosomes are acrocentric, and we reasoned they might undergo nondisjunction events at higher frequency. Chromosome numbers were assessed per nucleus, rather than per cell, as the protocol involved cell lysis. Among T5-1 cells, knockdown lymphoblast clone 1 (KL1) demonstrated statistically significant increased numerical abnormalities for chromosomes 13 and 21 individually. Abnormalities ranged from absence of a chromosome to the presence of as many as seven copies of a particular chromosome. Knockdown lymphoblast clone 2 (KL2) trended toward an increase in numerical chromosomal abnormalities. For both lines, numbers of nuclei with tetrasomy of either chromosome were statistically significant, with a ratio of 3:1 for knockdown to control. Among 82-6HT, knockdown fibroblast clone 2 (KF2) demonstrated statistically significant increased numerical chromosomal abnormalities, with tetrasomy for either chromosome 13 or 21 being the most commonly seen aberration; other abnormalities of number were also observed, but no cell had more than four copies of either chromosome. Knockdown fibroblast line 1 (KF1) did not demonstrate an increase in numerical aberrations by FISH (Fig. 5*C*). Thus, in three of the four diploid cell lines evaluated, across two different cell types, there was statistically significant induction of aneuploidy caused by depletion of KLHDC8B. Notably, the propensity for tetrasomy appears to correlate with tetraploidy and near-tetraploidy as common cytogenetic abnormalities in HL.

TABLE 4
Correlation of multinucleation and centrosomal amplification

	Multinuclear	Multinuclear, centrosomal amplification	% amplified	Mononuclear	Mononuclear, centrosomal amplification	% amplified
HeLa	12	6	50	788	7	0.89
FuKG1	13	7	53.8	587	5	0.85
FuKG22	21	6	28.6	579	8	1.38
Total, controls	46	19	41.3	1954	20	**1.02**[a]
FuKG10	58	31	53.4	342	15	4.39
FuKG19	50	33	66	550	23	4.18
Total, FuKG expressors	108	64	59.3	892	38	**4.26**[a]

[a] *p* value shows higher percentage of centrosomal amplification in mononuclear expressor cells *versus* mononuclear nonexpressor cells = 0.0001 (boldface values).

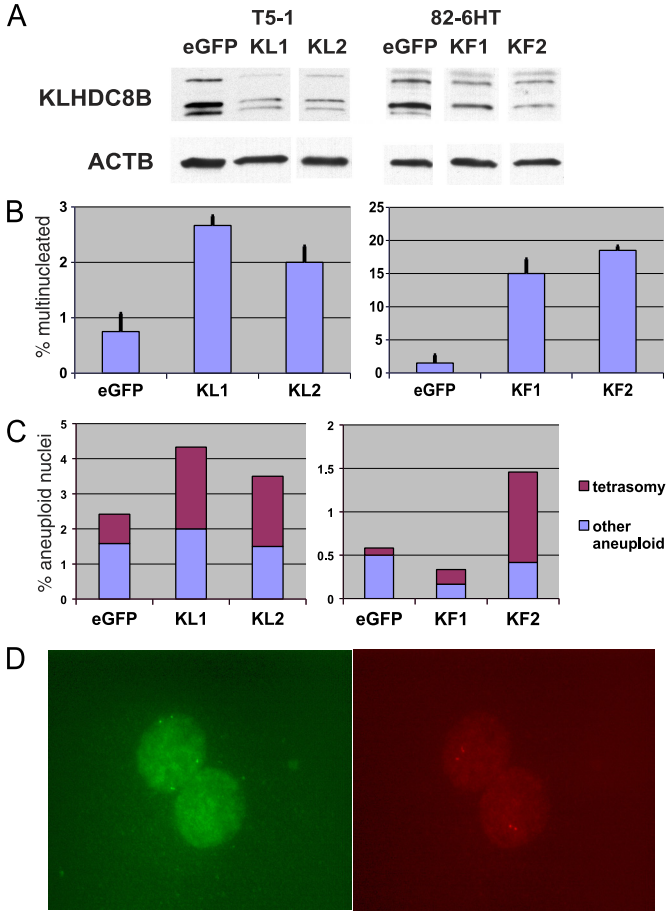

FIGURE 5. **Stable knockdown of KLHDC8B in diploid lymphoblasts and fibroblasts leads to multinucleation and aneuploidy.** *A,* Western blots of KLHDC8B expression in knockdown T5-1 lymphoblasts and 82-6HT fibroblasts. Cell lines were plated or subcultivated at low density and harvested after 48 h of growth. Enhanced GFP (*eGFP*) controls carried plasmid TR30003, containing an anti-GFP shRNA. *KL* and *KF* refer to knockdown lymphoblasts and knockdown fibroblasts, respectively; knockdown lines carried plasmid TI369559, containing an anti-KLHDC8B shRNA. *B,* cells were plated at low density to ensure optimal growth and harvested at 72 h. 800 cells were counted for each line, with the exception of KL1 (n = 600). *C,* FISH analysis of chromosomes 13 and 21 demonstrates increased aneuploidy among cell lines KL1, KL2, and KF2, compared with enhanced GFP controls. Tetrasomy (*crimson*) was the predominant chromosomal abnormality seen. 1200 cells were counted for each line. *p* values for aneuploidy relative to enhanced GFP control were as follows: *KL1*, $p = 0.01$; *KL2*, $p = 0.15$; *KF1*, $p = 0.55$; *KF2*, $p = 0.02$. *p* values for any tetrasomy relative to enhanced GFP control were as follows: KL1, $p = 0.004$; KL2, $p = 0.02$; KF1, $p = 1$; KF2, $p = 0.005$. *D,* image of FISH hybridization of two adjacent nuclei for line KL1. It is not discernible whether the nuclei originate from the same cell, a pair of daughter cells, or are associated randomly. The *upper left* nucleus demonstrates tetrasomy 13, and the *lower right* nucleus demonstrates complete loss of 13 (*green staining*). Both nuclei demonstrate disomy 21 (*red staining*).

DISCUSSION

The RS cell, of germinal center B lymphocyte origin, is the malignant cell of HL (2, 3). By interfering with the function of the midbody protein KLHDC8B, we reproduced the major pathologic features of the RS cell as follows: multinucleation, defective cytokinesis, centrosomal amplification, and aneuploidy. Using shRNA knockdown of KLHDC8B, we generated multinucleated B lymphoblasts that are morphologically similar to RS cells; we also induced aneuploidy, in particular tetraploidy, in B lymphoblasts and fibroblasts by means of KLHDC8B knockdown. Expression of the dominant-negative KLHDC8B-GFP fusion protein resulted in defective cytokinesis, with multiple instances of failed abscission, generation of anucleate daughter cells, and multipolar mitoses, providing potential mechanistic explanations for how RS cell morphology might arise. The presence of these alterations in several different derivative lines from multiple cell types, also seen in the FuKG cell lines, reinforces the validity of the findings and strongly argues against an off-target shRNA effect. The multinucleation data and live cell imaging provide evidence supporting the long held hypothesis that defective cytokinesis, rather than cell fusion, is responsible for the appearance of the RS cell (8, 9). Our data suggest that disruptions of mitotic mechanics play a central role in the pathogenesis of HL.

Aneuploidy, especially tetraploidy, and other chromosomal abnormalities are well documented in HL, pointing toward chromosomal instability as an underpinning of HL pathogenesis (11, 12, 16, 26). We present data suggesting that deficiency or malfunction of a midbody protein, in this case KLHDC8B, leads to failed cytokinesis and centrosomal amplification. In turn, centrosomal amplification increases the propensity of cells to missegregate individual chromosomes and perhaps even entire sets of chromosomes (*i.e.* nuclei). The results described were not limited to lymphoid cells, suggesting that the mechanism for chromosomal instability in HL may also be applicable to a variety of malignant and nonmalignant diseases characterized by defective midbody function. Interestingly, disruption of normal telomere length has also been shown to lead to similar anucleate cells in HL cell lines and is implicated in the transition from the Hodgkin cell to the RS cell, suggesting an alternate mechanism for mitotic errors that might lead to formation of the RS cell (20, 21, 27).

The KLHDC8B-GFP fusion protein (FuKG) appears to function as a dominant-negative mutant. The GFP fusion protein induces multinucleation more potently than depletion of KLHDC8B by RNAi. Stable transfectants, which produce small amounts of FuKG protein relative to native KLHDC8B, have a

profound effect on multinucleation and centrosomal amplification, presumably due to prolonged expression of the protein under selection pressure. Expression of FuKG replicates the effects of RNAi-mediated depletion of KLHDC8B, most notably multinucleation and centrosomal amplification, although it is not certain whether the effects of protein depletion and FuKG expression operate by the same mechanism. Occasional midbody localization of FuKG and perimitotic expression of FuKG support the notion of the dominant-negative role of FuKG. The fusion protein may interfere with normal functions of KLHDC8B. Those findings also suggest the possibility that aggregates of FuKG in the midzone region cause steric interference. There is recent evidence that dominant-negative mutations occur naturally in some types of kelch proteins and can be disease-causing; one example is KBTBD13, which is linked to nemaline rod myopathy (28).

KLHDC8B is one of 71 known or predicted human "kelch" family genes (29). Kelch proteins contain five to seven repeats of the ~50-amino acid kelch motif, coming together to form a β-propeller configuration (23); most kelch proteins contain additional domains, such as a "BTB/POZ" domain. KLHDC8B is one of only two kelch proteins containing seven kelch repeats and one of only seven lacking other recognizable domains. Kelch proteins participate in diverse biochemical activities, but a unifying theme is widespread participation in the machinery of cytokinesis (30). Participation in cytokinesis may be linked to the kelch domain's recognized ability to bind actin and participate in protein-protein interactions; the biochemical interactions of KLHDC8B are an intriguing topic for future exploration. KLHDC8B may not be unique in contributing to proper lymphoid development; the closely related BTB-kelch protein KLHL6 is necessary for B cell receptor signaling and germinal center formation (31).

Our results clarify the role of KLHDC8B in mitosis. KLHDC8B contributes to proper completion of abscission; this is consistent with our frequent video microscopic findings of failure to initiate or complete cleavage furrows. KLHDC8B may also contribute to the appropriate delivery of daughter nuclei to daughter cells, as evidenced by the significant number of anucleate cells generated by aberrant mitoses. Another kelch protein that localizes to the midzone, KLHL21, appears to be required for cytokinesis as well (32). BRCA2, most famous for its role in DNA damage control in the nucleus, localizes to the midbody; cell lines deficient in BRCA2 have difficulty completing cytokinesis and an increased fraction of binucleate cells (33). Thus, there is precedent for the behavior of KLHDC8B among midbody proteins. These observations are consistent with the hypothesis of Harvey (34) that binucleate cells arise by the failure of cell division after nuclear division. Cytokinesis failure alone increases the risk for tumorigenesis, due to the creation of tetraploid cells that are prone to chromosome missegregation and chromosomal rearrangements (35).

We observed a longer aggregate duration of mitosis with the dominant-negative protein FuKG. This delay, which is confined to cells undergoing aberrant mitoses, suggests activation of a checkpoint during mitosis (24). One example is the "mitotic checkpoint" during the metaphase-anaphase transition, which is triggered by unattached kinetochores and can delay anaphase for several hours (36). However, delayed or failed resolution of the midbody bridge accounts for the majority of the prolonged mitoses in our study. Similar outcomes have been demonstrated with depletion of BRCA2; multinucleated cells result, and cytokinesis is delayed (33, 37).

KLHDC8B plays a role in maintaining mitotic integrity, which likely is responsible for the findings of missegregation of chromosomes and even entire nuclei, which can occur in the presence of the dominant-negative FuKG. Other kelch domain-containing proteins may play similar roles. Keap1 appears to have a significant function in the midbody, where it locates during cytokinesis. RNA interference of Keap1 has been shown to contribute to multinucleation and chromosomal segregation defects in *Caenorhabditis elegans* (38). KLHL21 has been shown to associate with the chromosome passenger complex and aurora B (32), supporting the notion that different midbody kelch proteins can play essential roles in spindle checkpoint regulation and maintenance of chromosomal stability. As KLHDC8B lacks other recognizable functional domains (29), its range of intermolecular interactions may be more limited than those of BTB-Kelch proteins.

Centrosome amplification has been described in a variety of solid tumor and hematologic malignancies (39). Our results strongly imply that impaired midbody function or missing spindle checkpoint regulators can lead to centrosomal amplification in HL, although the mechanisms require further elucidation. Previous studies have also suggested that centrosomal amplification may arise independently of mitotic failure. It has been proposed that increased even numbers of centrosomes (*i.e.* 4, 6, 8, etc.) imply that mitotic failure is the driving force behind centrosomal amplification (40). We observed odd numbers, with three being predominant, in addition to even numbers (Fig. 4*B*), suggesting that KLHDC8B may have an impact on centrosome number outside of mitotic failure; a similar observation was made with centrosome amplification in endothelial cells (41). Nevertheless, KLHDC8B also seems to make a significant contribution to centrosomal amplification due to abscission failure, as centrosome number appeared correlated with multinucleation. Supernumerary centrosomes are known to cause multipolar mitoses and chromosome missegregation (18, 40, 42), suggesting a direct link between centrosome amplification and chromosomal instability, both of which are observed in our cell line models. We did find that multipolar mitoses were increased in the FuKG fusion protein expressors but were not present in large numbers. Malignant cells often have extra centrosomes but likely suppress multipolar mitoses as part of their survival strategy (43).

The strongest link between KLHDC8B and malignant transformation is the induction of aneuploidy upon knockdown. The estimated baseline rate of aneuploidy in human primary cells is about 0.01 per cell (44); the base-line rates of aneuploidy in our controls were roughly similar (0.005 per fibroblast and 0.02 per lymphoblast). KLHDC8B knockdown produced an approximate doubling in the numerical abnormalities of individual chromosomes. The increase was consistent across three cell lines in two different cell types and mirrors the increase in multinucleation seen with KLHDC8B depletion. Furthermore, increased rates of chromosomal aberrations such as aneuploidy

and micronuclei are associated with increased risk of cancer (45). Aneuploidy due to either loss or overexpression of spindle checkpoint proteins has been linked to tumorigenesis in studies of the kinetochore-localized protein kinases BUB1 and BUB1B (46, 47). In addition, the most common cytogenetic abnormality induced by KLHDC8B knockdown, tetrasomy, correlates with the tetraploid changes frequently seen in HL (13, 14). Findings of aneuploidy in response to KLHDC8B knockdown are thus consistent with results from other midbody proteins, although midbody proteins may impact chromosomal stability by playing roles that extend beyond regulation of abscission.

The accumulation of whole-genome sequencing data from individual malignancies has led to the identification of major pathways susceptible to tumor-inducing mutations (48). Twelve major groups of genes were referenced in the initial study. We suggest that mitotic and spindle checkpoint proteins should also be considered one of the key susceptible pathways, as demonstrated by the mounting body of evidence elucidating the roles of kelch and other functionally analogous proteins (30). Continued study of proteins such as KLHDC8B is demonstrating how genes encoding the cytokinetic machinery contribute to faithful cell division and segregation of chromosomes. KLHDC8B and other midbody proteins represent a significant category of albeit underappreciated tumor suppressors; the revelation of their mechanisms of action continues to bear out the hypotheses laid down many decades ago by pioneers such as Boveri (49) and Harvey (34).

Acknowledgments—We extend appreciation to Ron Seifert of the Garvey Imaging Lab for generous assistance with imaging techniques, Jacob Berman for technical support, and Stanley Gartler for discussions. T5-1 lymphoblasts were a gift of Kimberly Muczynski. 82-6HT fibroblasts were a gift of Peter Rabinovitch.

REFERENCES

1. Siegel, R., Naishadham, D., and Jemal, A. (2012) Cancer statistics. *CA-Cancer J. Clin.* **62,** 10–29
2. Küppers, R. (2009) The biology of Hodgkin lymphoma. *Nat. Rev. Cancer* **9,** 15–27
3. Re, D., Küppers, R., and Diehl, V. (2005) Molecular pathogenesis of Hodgkin lymphoma. *J. Clin. Oncol.* **23,** 6379–6386
4. Kanzler, H., Küppers, R., Hansmann, M. L., and Rajewsky, K. (1996) Hodgkin and Reed-Sternberg cells in Hodgkin disease represent the outgrowth of a dominant tumor clone derived from (crippled) germinal center B cells. *J. Exp. Med.* **184,** 1495–1505
5. Küppers, R., Rajewsky, K., Zhao, M., Simons, G., Laumann, R., Fischer, R., and Hansmann, M. L. (1994) Hodgkin disease. Hodgkin and Reed-Sternberg cells picked from histological sections show clonal immunoglobulin gene rearrangements and appear to be derived from B cells at various stages of development. *Proc. Natl. Acad. Sci. U.S.A.* **91,** 10962–10966
6. Marafioti, T., Hummel, M., Foss, H. D., Laumen, H., Korbjuhn, P., Anagnostopoulos, I., Lammert, H., Demel, G., Theil, J., Wirth, T., and Stein, H. (2000) Hodgkin and Reed-Sternberg cells represent an expansion of a single clone originating from a germinal center B cell with functional immunoglobulin gene rearrangements but defective immunoglobulin transcription. *Blood* **95,** 1443–1450
7. Drexler, H. G., Gignac, S. M., Hoffbrand, A. V., and Minowada, J. (1989) Formation of multinucleated cells in a Hodgkin disease-derived cell line. *Int. J. Cancer* **43,** 1083–1090
8. Küppers, R., Bräuninger, A., Müschen, M., Distler, V., Hansmann, M. L., and Rajewsky, K. (2001) Evidence that Hodgkin and Reed-Sternberg cells in Hodgkin disease do not represent cell fusions. *Blood* **97,** 818–821
9. Leoncini, L., Spina, D., Megha, T., Gallorini, M., Tosi, P., Hummel, M., Stein, H., Pileri, S., Kraft, R., Laissue, J. A., and Cottier, H. (1997) Cell kinetics, morphology, and molecular IgVH gene rearrangements in Hodgkin disease. *Leuk. Lymphoma* **26,** 307–316
10. Newcom, S. R., Kadin, M. E., and Phillips, C. (1988) L-428 Reed-Sternberg cells and mononuclear Hodgkin cells arise from a single cloned mononuclear cell. *Int. J. Cell Cloning* **6,** 417–431
11. Barrios, L., Caballín, M. R., Mirò, R., Fuster, C., Berrozpe, G., Subías, A., Batlle, X., and Egozcue, J. (1988) Chromosome abnormalities in peripheral blood lymphocytes from untreated Hodgkin's patients. A possible evidence for chromosome instability. *Hum. Genet.* **78,** 320–324
12. M'kacher, R., Girinsky, T., Koscielny, S., Dossou, J., Violot, D., Béron-Gaillard, N., Ribrag, V., Bourhis, J., Bernheim, A., Parmentier, C., and Carde, P. (2003) Base line and treatment-induced chromosomal abnormalities in peripheral blood lymphocytes of Hodgkin lymphoma patients. *Int. J. Radiat. Oncol. Biol. Phys.* **57,** 321–326
13. Falzetti, D., Crescenzi, B., Matteuci, C., Falini, B., Martelli, M. F., Van Den Berghe, H., and Mecucci, C. (1999) Genomic instability and recurrent breakpoints are main cytogenetic findings in Hodgkin disease. *Haematologica* **84,** 298–305
14. Watanabe, A., Inokuchi, K., Yamaguchi, H., Mizuki, T., Tanosaki, S., Shimada, T., and Dan, K. (2004) Near-triploidy and near-tetraploidy in hematological malignancies and mutation of the p53 gene. *Clin. Lab. Haematol.* **26,** 25–30
15. Krämer, A., Schweizer, S., Neben, K., Giesecke, C., Kalla, J., Katzenberger, T., Benner, A., Müller-Hermelink, H. K., Ho, A. D., and Ott, G. (2003) Centrosome aberrations as a possible mechanism for chromosomal instability in non-Hodgkin lymphoma. *Leukemia* **17,** 2207–2213
16. Martín-Subero, J. I., Knippschild, U., Harder, L., Barth, T. F., Riemke, J., Grohmann, S., Gesk, S., Höppner, J., Möller, P., Parwaresch, R. M., and Siebert, R. (2003) Segmental chromosomal aberrations and centrosome amplifications. Pathogenetic mechanisms in Hodgkin and Reed-Sternberg cells of classical Hodgkin lymphoma? *Leukemia* **17,** 2214–2219
17. Pihan, G. A., Purohit, A., Wallace, J., Knecht, H., Woda, B., Quesenberry, P., and Doxsey, S. J. (1998) Centrosome defects and genetic instability in malignant tumors. *Cancer Res.* **58,** 3974–3985
18. Ganem, N. J., Godinho, S. A., and Pellman, D. (2009) A mechanism linking extra centrosomes to chromosomal instability. *Nature* **460,** 278–282
19. Re, D., Zander, T., Diehl, V., and Wolf, J. (2002) Genetic instability in Hodgkin lymphoma. *Ann. Oncol.* **13,** 19–22
20. Knecht, H., Sawan, B., Lichtensztejn, D., Lemieux, B., Wellinger, R. J., and Mai, S. (2009) The 3D nuclear organization of telomeres marks the transition from Hodgkin to Reed-Sternberg cells. *Leukemia* **23,** 565–573
21. Martínez, P., and Blasco, M. A. (2011) Telomeric and extra-telomeric roles for telomerase and the telomere-binding proteins. *Nat. Rev. Cancer* **11,** 161–176
22. Salipante, S. J., Mealiffe, M. E., Wechsler, J., Krem, M. M., Liu, Y., Namkoong, S., Bhagat, G., Kirchhoff, T., Offit, K., Lynch, H., Wiernik, P. H., Roshal, M., McMaster, M. L., Tucker, M., Fromm, J. R., Goldin, L. R., Horwitz, M. S. (2009) Mutations in a gene encoding a midbody kelch protein in familial and sporadic classical Hodgkin lymphoma lead to binucleated cells. *Proc. Natl. Acad. Sci. U.S.A.* **106,** 14920–14925
23. Adams, J., Kelso, R., and Cooley, L. (2000) The kelch repeat superfamily of proteins. Propellers of cell function. *Trends Cell Biol.* **10,** 17–24
24. Rieder, C. L. (2011) Mitosis in vertebrates. The G_2/M and M/A transitions and their associated checkpoints. *Chromosome Res.* **19,** 291–306
25. Storkus, W. J., Alexander, J., Payne, J. A., Dawson, J. R., and Cresswell, P. (1989) Reversal of natural killing susceptibility in target cells expressing transfected class I HLA genes. *Proc. Natl. Acad. Sci. U.S.A.* **86,** 2361–2364
26. Guffei, A., Sarkar, R., Klewes, L., Righolt, C., Knecht, H., and Mai, S. (2010) Dynamic chromosomal rearrangements in Hodgkin lymphoma are due to ongoing three-dimensional nuclear remodeling and breakage-bridge fusion cycles. *Haematologica* **95,** 2038–2046
27. Knecht, H., Brüderlein, S., Wegener, S., Lichtensztejn, D., Lichtensztejn, Z., Lemieux, B., Möller, P., and Mai, S. (2010) 3D nuclear organization of telomeres in the Hodgkin cell lines U-HO1 and U-HO1-PTPN1. PTPN1 expression prevents the formation of very short telomeres including

"t-stumps." *BMC Cell Biol.* **11,** 99–108
28. Sambuughin, N., Yau, K. S., Olivé, M., Duff, R. M., Bayarsaikhan, M., Lu, S., Gonzalez-Mera, L., Sivadorai, P., Nowak, K. J., Ravenscroft, G., Mastaglia, F. L., North, K. N., Ilkovski, B., Kremer, H., Lammens, M., van Engelen, B. G., Fabian, V., Lamont, P., Davis, M. R., Laing, N. G., and Goldfarb, L. G. (2010) Dominant mutations in KBTBD13, a member of the BTB/Kelch family, cause nemaline myopathy with cores. *Am. J. Hum. Genet.* **87,** 842–847
29. Prag, S., and Adams, J. C. (2003) Molecular phylogeny of the kelch-repeat superfamily reveals an expansion of BTB/kelch proteins in animals. *BMC Bioinformatics* **4,** 42–61
30. Krem, M. M., Salipante, S. J., and Horwitz, M. S. (2010) Mutations in a gene encoding a midbody protein in binucleated Reed-Sternberg cells of Hodgkin lymphoma. *Cell Cycle* **9,** 670–675
31. Kroll, J., Shi, X., Caprioli, A., Liu, H. H., Waskow, C., Lin, K. M., Miyazaki, T., Rodewald, H. R., and Sato, T. N. (2005) The BTB-kelch protein KLHL6 is involved in B-lymphocyte antigen receptor signaling and germinal center formation. *Mol. Cell. Biol.* **25,** 8531–8540
32. Maerki, S., Olma, M. H., Staubli, T., Steigemann, P., Gerlich, D. W., Quadroni, M., Sumara I., and Peter, M. (2009) The Cul3-KLHL21 E3 ubiquitin ligase targets aurora B to midzone microtubules in anaphase and is required for cytokinesis. *J. Cell Biol.* **187,** 791–800
33. Daniels, M. J., Wang, Y., Lee, M., and Venkitaraman, A. R. (2004) Abnormal cytokinesis in cells deficient in the breast cancer susceptibility protein BRCA2. *Science* **306,** 876–879
34. Harvey, E. B. (1919) Mitotic division of binucleate cells. *Biol. Bull.* **37,** 96–100
35. Fujiwara, T., Bandi, M., Nitta, M., Ivanova, E. V., Bronson, R. T., and Pellman, D. (2005) Cytokinesis failure generating tetraploids promotes tumorigenesis in p53-null cells. *Nature* **437,** 1043–1047
36. Rieder, C. L., Schultz, A., Cole, R., and Sluder, G. (1994) Anaphase onset in vertebrate somatic cells is controlled by a checkpoint that monitors sister kinetochore attachment to the spindle. *J. Cell Biol.* **127,** 1301–1310
37. Jonsdottir, A. B., Vreeswijk, M. P., Wolterbeek, R., Devilee, P., Tanke, H. J., Eyfjörd, J. E., and Szuhai, K. (2009) BRCA2 heterozygosity delays cytokinesis in primary human fibroblasts. *Cell Oncol.* **31,** 191–201
38. Skop, A. R., Liu, H., Yates, J., 3rd, Meyer, B. J., and Heald, R. (2004) Dissection of the mammalian midbody proteome reveals conserved cytokinesis mechanisms. *Science* **305,** 61–66
39. Zyss, D., and Gergely, F. (2009) Centrosome function in cancer. Guilty or innocent? *Trends Cell Biol.* **19,** 334–346
40. Lingle, W. L., Lukasiewicz, K., and Salisbury, J. L. (2005) Deregulation of the centrosome cycle and the origin of chromosomal instability in cancer. *Adv. Exp. Med. Biol.* **570,** 393–421
41. Taylor, S. M., Nevis, K. R., and Park, H. L. (2010) Angiogenic factor signaling regulates centrosome duplication in endothelial cells of developing blood vessels. *Blood* **116,** 3108–3117
42. Conery, A. R., and Harlow, E. (2010) High throughput screens in diploid cells identify factors that contribute to the acquisition of chromosomal instability. *Proc. Natl. Acad. Sci. U.S.A.* **107,** 15455–15460
43. Godinho, S. A., Kwon, M., and Pellman, D. (2009) Centrosomes and cancer. How cancer cells divide with too many centrosomes. *Cancer Metastasis Rev.* **28,** 85–98
44. Schwartz, J. L., Jordan, R., Evans, H. H., Lenarczyk, M., and Liber, H. L. (2004) Base-line levels of chromosome instability in the human lymphoblastoid cell TK6. *Mutagenesis* **19,** 477–482
45. Norppa, H. (2004) Cytogenetic biomarkers. *IARC Sci. Publ.* **157,** 179–205
46. Hanks, S., Coleman, K., Reid, S., Plaja, A., Firth, H., Fitzpatrick, D., Kidd, A., Méhes, K., Nash, R., Robin, N., Shannon, N., Tolmie, J., Swansbury, J., Irrthum, A., Douglas, J., and Rahman, N. (2004) Constitutional aneuploidy and cancer predisposition caused by biallelic mutations in BUB1B. *Nat. Genet.* **36,** 1159–1161
47. Matsuura, S., Matsumoto, Y., Morishima, K., Izumi, H., Matsumoto, H., Ito, E., Tsutsui, K., Kobayashi, J., Tauchi, H., Kajiwara, Y., Hama, S., Kurisu, K., Tahara, H., Oshimura, M., Komatsu, K., Ikeuchi, T., and Kajii, T. (2006) Monoallelic BUB1B mutations and defective mitotic-spindle checkpoint in seven families with premature chromatid separation (PCS) syndrome. *Am. J. Med. Genet. A* **140,** 358–367
48. Jones, S., Zhang, X., Parsons, D. W., Lin, J. C., Leary, R. J., Angenendt, P., Mankoo, P., Carter, H., Kamiyama, H., Jimeno, A., Hong, S. M., Fu, B., Lin, M. T., Calhoun, E. S., Kamiyama, M., Walter, K., Nikolskaya, T., Nikolsky, Y., Hartigan, J., Smith, D. R., Hidalgo, M., Leach, S. D., Klein, A. P., Jaffee, E. M., Goggins, M., Maitra, A., Iacobuzio-Donahue, C., Eshleman, J. R., Kern, S. E., Hruban, R. H., Karchin, R., Papadopoulos, N., Parmigiani, G., Vogelstein, B., Velculescu, V. E., and Kinzler, K. W. (2008) Core signaling pathways in human pancreatic cancers revealed by global genomic analyses. *Science* **321,** 1801–1806
49. Boveri, T. (1914) *Zur Frage der Entstehung Maligner Tumor,* Fischer Verlag, Jena, Germany (English translation by M. Boveri (1929) reprinted as *The Origin of Malignant Tumors,* Williams and Wilkins, Baltimore)